Original Article

Feasibility of using 8 mL of iodinated contrast media in cerebral computed tomographic angiography with a dual-layer spectral detector

Yinping Leng[1#], Ying Liu[1#], Shuhao Li[1], Xiwen Wang[1], Weiwei Deng[2], Yu Wang[2], Lianggeng Gong[1]

[1]Department of Radiology, the Second Affiliated Hospital of Nanchang University, Nanchang, China; [2]Clinical and Technical Support, Philips Healthcare, Shanghai, China

Contributions: (I) Conception and design: Y Leng, L Gong; (II) Administrative support: L Gong; (III) Provision of study materials or patients: X Wang, Y Liu; (IV) Collection and assembly of data: S Li, Y Liu; (V) Data analysis and interpretation: Y Wang, W Deng; (VI) Manuscript writing: All authors; (VII) Final approval of manuscript: All authors.

[#]These authors contributed equally to this work.

Correspondence to: Lianggeng Gong, PhD. Department of Radiology, the Second Affiliated Hospital of Nanchang University, No. 1 Minde Road, Nanchang 330006, China. Email: gong111999@126.com.

Background: Virtual monoenergetic images (VMIs) at a low energy level can improve image quality when the amount of iodinated contrast media (CM) is reduced. The purpose was to evaluate the feasibility of using an extremely low CM volume and injection rate in cerebral computed tomography angiography (CTA) on a dual-layer spectral detector computed tomography (CT).

Methods: Patients who were clinically suspected of intracranial aneurysm or cerebrovascular diseases were included in our study (from June to November 2022). In this prospective study, 80 patients were randomly enrolled into group A (8 mL of CM with a 1-mL/s flow rate) or group B (40 mL of CM with 4-mL/s flow rate). The VMIs at 40–70 keV in group A and polychromatic conventional images in the 2 groups were reconstructed. CT attenuation, image noise, contrast-to-noise ratio (CNR), and signal-to-noise ratio (SNR) were evaluated via the *t*-test or Mann-Whitney test (2 groups), while analysis of variance or Kruskal-Wallis test (multiple groups). Subjective image quality was assessed on a 5-point scale.

Results: In group A, the subjective image quality score, CT attenuation, and CNR of the internal carotid artery (ICA) and middle cerebral artery (MCA) were the highest on VMIs at 40 keV. The image noise on VMIs at 40 keV was 5.08±0.84 Hounsfield units. The subjective image quality score, CT value of the ICA, MCA, and cerebral parenchyma on VMIs at 40 keV in group A were similar to those in group B (all P values >0.05). Compared to those in group B, the VMIs at 40 keV in group A demonstrated a significantly higher mean SNR and CNR of the ICA (mean SNR: 46.22±20.18 *vs.* 34.32±12.40, P=0.002; CNR: 55.47±13.43 *vs.* 46.18±12.30, P=0.002) and MCA [SNR: 13.66 (9.78, 20.29) *vs.* 9.99 (7.53, 14.00), P=0.003; CNR: 47.00±12.71 *vs.* 39.45±10.47, P=0.005].

Conclusions: Cerebral CTA on VMIs at 40 keV with 8 mL of CM and a 1-mL/s injection rate can provide diagnostic image quality.

Keywords: Cerebral; contrast media (CM); spectral detector computed tomography (SDCT); computed tomography angiography (CTA); virtual monoenergetic image (VMI)

Introduction

Computed tomography angiography (CTA) has higher sensitivity and specificity than does magnetic resonance imaging in detecting small intracranial aneurysms and displaying calcification of an aneurysm wall or thrombus within the lumen of an aneurysm (1-3). Therefore, CTA is being increasingly applied to the examination of suspected cerebrovascular diseases, especially in multiple follow-ups and reexaminations after the aneurysm operation. However, some potential hazards, such as iodine adverse events or the kidney damage, may occur when the volume and injection rate of the iodinated contrast media (CM) are high. These potential hazards are sometimes fatal for or older patients or those with renal insufficiency, hypovolemia, diabetes mellitus (4-7). Contrast-associated acute kidney injury (CA-AKI) is an acute kidney injury caused by iodinated CM, with short-term and long-term adverse outcomes (7). In order to reduce this injury, some researchers have tried to reduce the CM dose (8-11). One study reported that cerebral CTA at 70 kVp can reduce the CM dose by approximately 50% while ensuring diagnostic image quality (11). However, the use of a low tube voltage to reduce CM dose may lead to an increase in noise, thus damaging the image quality.

Dual-layer spectral detector computed tomography (SDCT) adopts a single-source dual-detector imaging mode and simultaneously measures high-energy and low-energy projection data in 2 detector layers at the same space and angular position (12-15). SDCT uses an anticorrelation noise reduction algorithm to maintain low noise in all energy levels of virtual monoenergetic images (VMIs) (16-18). Virtual monochrome reconstruction at low energy can improve image quality (19). It has been found that under the low-energy VMIs of SDCT, reducing the CM dose of coronary and run-off CTA can ensure the diagnosability of image quality (20-23). Therefore, we assumed that using extremely low CM volume with a lower kiloelectron voltage (keV) of VMIs from SDCT would not degrade the image quality in cerebral CTA.

This study aimed to evaluate the feasibility of using 8 mL of CM and a 1-mL/s injection rate with VMIs for cerebral CTA from SDCT and to identify the optimal VMIs for clinical application.

Methods

Patients

This study was conducted in accordance with the Declaration of Helsinki (as revised in 2013) and was approved by the Institutional Review Board of The Second Affiliated Hospital of Nanchang University (examination and approval number review No. 2022 [054]). Informed consent was obtained from all individual participants.

Patients who were clinically suspected of intracranial aneurysm or cerebrovascular diseases, had previous subarachnoid hemorrhage, and were offered further treatment were included in our study (from June to November 2022). The exclusion criteria were as follows: patients with renal insufficiency, with contraindications to iodinated CM, and with motion artifacts. Finally, 40 patients were randomly enrolled into experimental group A (8 mL of CM with a flow rate of 1 mL/s) and then matched with the same number of cases in control group B (40 mL of CM with a flow rate of 4 mL/s). We recorded the height and weight of each patient before the CTA examination and calculated the body mass index (BMI).

Images acquisition

All patients underwent cerebral CTA examinations on a dual-layer spectral detector (IQon, Philips Healthcare, Amsterdam, the Netherlands). The parameters of the cerebral CTA scheme in our study were as follows: detector collimation, 64×0.625 mm; gantry rotation time, 0.4 s; helical pitch, 1.21; matrix, 512×512; tube voltage, 120 kVp; and automated tube current. The iodinated CM used was 400 mgI/mL of iomeprol (Bracco, Milan, Italy), which was injected through the antecubital vein with a high-pressure syringe (Ulrich Medical, Ulm, Germany). In group A, the volume of CM was 8 mL, which was injected intravenously at a flow rate of 1 mL/s and was followed by a saline injection of 30 mL at a flow rate of 3 mL/s. In group B, the volume of CM was 40 mL, which was injected intravenously at a flow rate of 4 mL/s and was followed by a saline injection of 40 mL at 5 mL/s. The start time of data acquisition was determined by using a computer-assisted bolus-tracking technique, with the region of interest (ROI) placed in the cervical segment of the internal carotid artery (ICA) about the level of the first cervical vertebra. In group A, when the computed tomography (CT) attenuation value of ROI increased by more than 20 Hounsfield units (HU) relative to plain scanning data acquisition was triggered manually 3 seconds after this threshold was reached. In group B, the triggering threshold of the ICA was 150 HU, and data collection began 3 seconds after triggering.
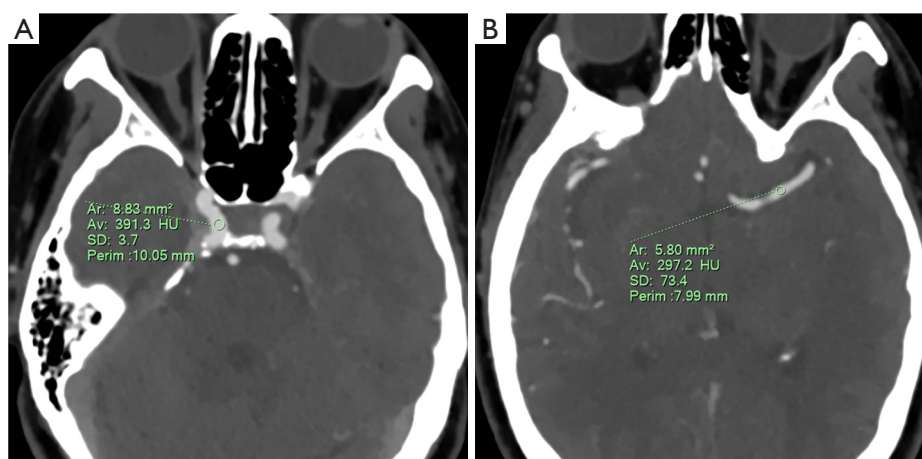
Figure 1 The ROI in the target vessels. Multiplanar reconstruction (thin section, axial) contrast-enhanced CT images: (A) an ROI placed in the cavernous segment of the internal carotid artery and (B) an ROI placed in the first segment of the middle cerebral artery. Window settings: level 700 HU and width 1,900 HU. Ar, area; Av, average value; HU, Hounsfield unit; SD, standard deviation; Perim, perimeter; ROI, region of interest; CT, computed tomography.

Image reconstruction

Spectral-based images (SBIs) in group A and polychromatic conventional images (PCIs) in both groups were generated and then transferred to a commercial workstation (IntelliSpace Portal Version 10.0, Philips Healthcare) for image analysis. VMIs at high energy can effectively inhibit the artifacts of wire harness hardening but simultaneously reduce the tissue contrast of blood vessels. The CT attenuation value of VMIs at 65–70 keV is approximately equivalent to the attenuation obtained from single-energy CT scans at 120 kVp (24). Finally, VMIs from 40 to 70 keV (VMI 40 to 70 keV) with a 10-keV increment were reconstructed from SBIs in group A. The reconstruction parameters were as follows: a spectral reconstruction algorithm (Spectral, filter B, level 3, Philips Healthcare) for VMIs in group A, a hybrid iterative reconstructive algorithm (iDose[4], level 3) for PCIs in both groups, a slice thickness of 1 mm, and an increment of 0.5 mm.

Objective image quality evaluation

An experienced neuroradiologist with 7 years of cerebral CTA experience completed all objective measurement assessments. All objective measurements were made in the multiplanar reconstruction (thin-section axial CT) image mode. We chose the cavernous segment of the ICA and the first segment of middle cerebral artery (MCA) as the ROIs (9) (*Figure 1*). All ROIs were placed in uniform areas,

and the sizes were selected to be about two-thirds of the cross-sectional area of the target vessel, with no contact being made with the vessel wall or calcified plaque. The average CT attenuation values were obtained by measuring the bilateral ICA and MCA 3 times, and the corresponding standard deviation (SD) was recorded. The CT values of the cerebral parenchyma were obtained by placing an ROI with an area of approximate 1 cm^2 in the centrum semiovale. The CT values of the cerebral parenchyma were measured 3 times, with the vascular structures being avoided. Image noise was regarded as the SD of the CT numbers in the cerebral parenchyma. We used the following formulae to calculate the signal-to-noise ratio (SNR) and contrast-to-noise ratio (CNR) (9):

$$SNR = CT\ attenuation_a\ /\ SD_a \qquad [1]$$

$$CNR = \left(CT\ attenuation_a - CT\ attenuation_b\right) / SD \qquad [2]$$

where CT attenuation$_a$ is the average CT attenuation of the ICA or MCA, SD$_a$ is the SD of the CT attenuation in the ICA or MCA, CT attenuation$_b$ is the average CT attenuation of the cerebral parenchyma, and SD is the image noise.

Pre-experiment

Before the formal implementation of this study, we attempted to perform cerebral CTA scans by administering

Table 1 Subjective image quality evaluation parameters and 5-point score

Score	Image noise	Vessel sharpness	Contrast	Diagnostic image quality
5	No noise	Sharp edges	High contrast	Excellent diagnostic confidence
4	Low noise	Minimal blurred edges	Good contrast	Good diagnostic confidence
3	Mild noise	Mild blurred edges	Medium contrast	Acceptable diagnostic confidence
2	Increased noise	Increased blurred edges	Light contrast	Limited diagnostic confidence
1	Obvious noise	Obvious blurred edges	Poor contrast	No diagnostic confidence

different volumes of CM (20, 10, 8, and 7 mL). There were 5 patients in each group, with corresponding injection rates of 2.5, 1.2, 1, and 0.8 mL/s. The triggering algorithm and reconstruction parameters were the same as those of the experimental group, and the VMI 40 keV was reconstructed. The CT value, CNR and SNR of the ICA, and image noise were measured at VMI 40 keV, and the subjective scores of image quality were recorded.

Subjective image quality evaluation

The images were reviewed on maximum intensity projection to evaluate subjective image quality. The subjective image quality was assessed independently and completed by 2 neuroradiologists with 7 and 5 years of CTA reading experience, respectively. The 2 doctors were blinded to the patient's characteristics, medical history, and reconstruction technology. The subjective image quality of cerebral CTA was assessed on a 5-point scale (10). The window settings were adjusted to evaluate the optimal subjective image quality. A detailed description of the subjective scoring criteria is summarized in *Table 1*.

Radiation dose analysis

The volume CT dose index (CTDIvol) and dose-length product (DLP) were recorded for each patient. CTDIvol was used to evaluate the average dose received by the patient per unit volume during scanning, and DLP was the total radiation dose needed for the patient to complete a CT examination. The effective dose (ED) was calculated by multiplying the DLP with the International Commission on Radiological Protection conversion coefficient for head CT imaging (0.0021) (25).

Statistical analysis

Statistical analysis of all data was performed with SPSS

26.0 (IBM Corp., Armonk, NY, USA). Quantitative data conforming to the normal distribution are expressed as the mean ± SD, and the *t*-test was used for the comparison between groups; meanwhile, quantitative data with a nonnormal distribution are expressed as medians with interquartile ranges, and the Mann-Whitney test was used for comparison. Qualitative data were compared by using the chi-squared test or Fisher exact test. Quantitative data between multiple groups that followed a normal distribution were compared using analysis of variance. Quantitative data between multiple groups that followed a nonnormal distribution were compared using the Kruskal-Wallis test. Subjective image quality scores were compared with the Mann-Whitney test for 2 groups and with the Kruskal-Wallis test for multiple groups. Differences were considered statistically significant at a P value<0.05. The kappa consistency test was used to assess the interreader agreement for the evaluation of subjective image quality. κ values indicated the following: less than 0.20, poor consistency; 0.21–0.40, fair consistency; 0.41–0.60, moderate consistency; a 0.61–0.80, good consistency; and 0.81–1.00, almost perfect consistency (8).

Results

Patient population and radiation dose

The patient characteristics and radiation doses are shown in *Table 2*. Overall, 80 patients were included in this study, with 40 each in group A and group B. Group A included 18 males and 22 females, with a mean age of 56.3±12.96 years (range, 29–81 years). Group B included 20 males and 20 females, with an average age of 58.48±14.42 years (range, 26–85 years). There were no significant differences in age, sex, weight, height, or BMI between the groups (all P values >0.05). The DLP, CTDIvol, and ED showed no significant differences between the 2 groups (P>0.05). No CM-related adverse reactions occurred in any of the patients after the

Table 2 Patient characteristics and radiation doses

Item	Group A (n=40)	Group B (n=40)	P value
Sex (male/female)	18/22	20/20	0.654[†]
Age (years)	56.3±12.96 [29–81]	58.48±14.42 [26–85]	0.480[‡]
Height (cm)	166.85±7.44 [154–179]	168.20±8.38 [156–183]	0.593[‡]
Weight (kg)	64.23±11.75 [48.2–94.2]	66.55±11.88 [48.2–90.7]	0.538[‡]
BMI (kg/m^2)	22.96±3.05 [19.2–29.41]	23.38±2.80 [19.8–28.73]	0.653[‡]
CTDIvol (mGy)	36 [36, 36]	36 [36, 36]	>0.99[§]
DLP (mGy·cm)	795 [795, 831]	804 [777, 831]	0.906[§]
ED (mSv)	1.67 [1.67, 1.75]	1.69 [1.63, 1.75]	0.770[§]

Data are presented as the mean ± standard deviation [range] for normally distributed continuous variables and as the median [interquartile range] for nonnormally distributed continuous variables. Group A: 8 mL of CM with a 1-mL/s flow rate; group B: 40 mL of CM with 4-mL/s flow rate. [†], chi-squared test; [‡], *t*-test; [§], Mann-Whitney test. BMI, body mass index; CTDIvol, volume computed tomography dose index; DLP, dose-length product; ED, effective dose; CM, contrast media.

Table 3 Results of the pre-experiment

Volume of contrast media	20 mL	10 mL	8 mL	7 mL	P value
ICA					
CT value (HU)	715.08±114.68	353.82±76.16	315.19±53.33	224.20±44.81	<0.001[†]
SNR	83.78±20.20	60.23±33.00	50.42±6.73	26.66±10.32	0.017[†]
CNR	129.97±39.48	57.13±14.30	52.12±10.05	31.41±8.98	<0.001[†]
Cerebral parenchyma					
CT value (HU)	34.34±2.44	31.82±5.61	31.58±1.50	31.23±1.25	0.512[†]
Noise (HU)	5.42±1.01	5.88±1.67	5.5±0.91	6.20±0.35	0.772[†]
Mean subjective image quality score	5 [5, 5]	5 [4.5, 5]	5 [4, 5]	4 [3, 4]	0.026[‡]

Data are presented as the mean ± standard deviation for normally distributed continuous variables and as the median [interquartile range] for nonnormally distributed continuous variables. [†], analysis of Variance; [‡], Kruskal-Wallis test. ICA, internal carotid artery; CT, computed tomography; HU, Hounsfield unit; SNR, signal-to-noise ratio, CNR, contrast-to-noise ratio.

examination.

Pre-experiment analysis

The objective and subjective image quality analyses of 20, 10, 8, and 7 mL of CM are detailed in *Table 3*. In the subgroup of 8-mL CM volume, the average CT value of the ICA for VMIs$_{40 \text{ keV}}$ was 315.19±53.33 HU, SNR was 50.42±6.73, CNR was 52.12±10.05, noise was 5.5±0.91, and subjective score was 5 [4, 5]. When the CM volume was further reduced to 7 mL, the average CT value of the ICA for VMIs$_{40 \text{ keV}}$ was 224.20±44.81 HU, SNR was 26.66±10.32, CNR was 31.41±8.98, noise was 6.20±0.35 HU,

and subjective quality score was 4 [3, 4]. *Figure 2* displays an example of the pre-experiment maximum intensity projection images.

Objective image quality analysis

Table 4 shows the objective image quality analysis results in group A. In group A, the CT attenuation values of the ICA and MCA were significantly higher for VMIs$_{40–60 \text{ keV}}$ than those for PCIs (all P values <0.05), while there were no significant difference between the values of VMIs$_{70 \text{ keV}}$ and PCIs (P>0.99 and P=0.567). In group A, the CNR$_{ICA}$, CNR$_{MCA}$, and SNR$_{ICA}$ were significantly higher for
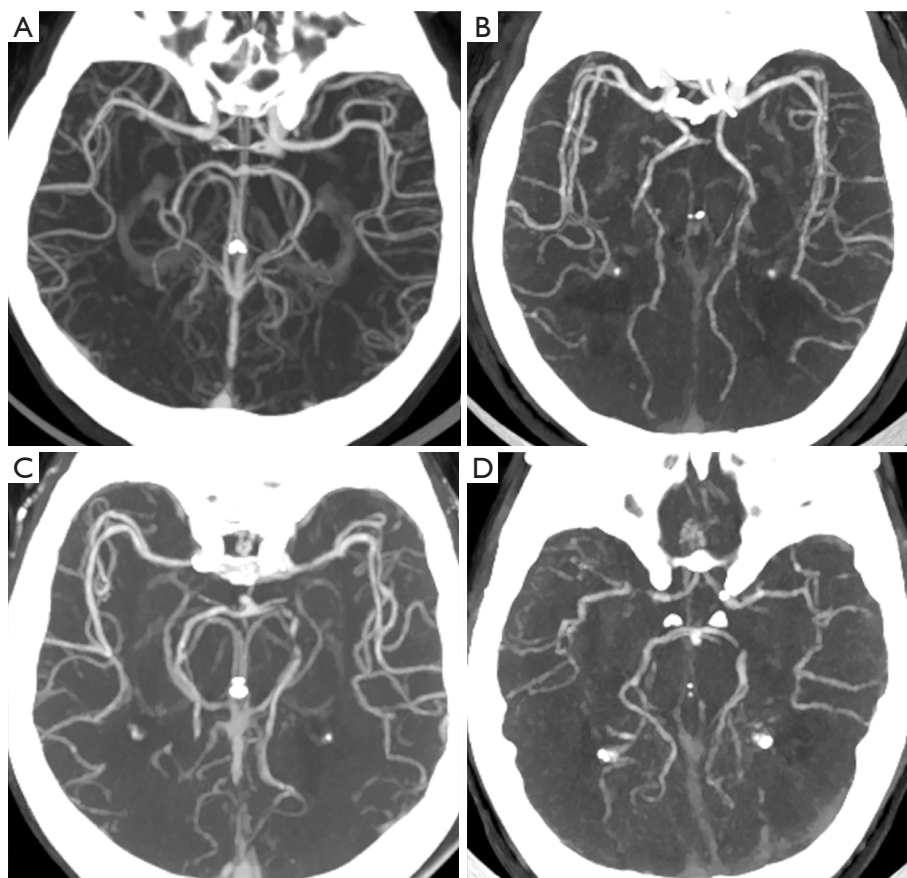
Figure 2 Example maximum intensity projection images of the pre-experiment. The images under (A) 20 mL of contrast media, (B)10 mL of contrast media, (C) 8 mL of contrast media, and (D) 7 mL of contrast media. Window settings: level 500 HU and width 1,000 HU. HU, Hounsfield unit.

$VMIs_{40-70 \text{ keV}}$ than those for PCIs (all P values <0.05). In group A, there was no significant difference in the SNR_{MCA} for $VMIs_{40-70 \text{ keV}}$ and for PCIs (all P values >0.05). In group A, the image noise was significantly higher for PCIs than for $VMIs_{40-70 \text{ keV}}$ (all P values <0.05), while VMIs at 50 keV exhibited a lower image noise compared to those at 40 keV (P<0.05). In group A, there was a progressive increase in the CT attenuation values and CNR of the ICA and MCA but a decrease in VMI levels, meaning that the CT attenuation and CNR were the highest on $VMIs_{40 \text{ keV}}$. Example axial images of VMIs (40–70 keV) and PCIs in group A are shown in *Figure 3*.

Table 5 summarizes the results of objective image quality analysis between the $VMIs_{40-\text{keV}}$ in group A and the PCIs in group B. The average CT attenuation values of ICA, MCA, and cerebral parenchyma on $VMIs_{40-\text{keV}}$ in group A were similar to those of the PCIs in group B (all P values >0.05).

The SNR_{ICA}, CNR_{ICA}, SNR_{MCA}, and CNR_{MCA} of group A ($VMI_{40 \text{ keV}}$) were significantly higher than those in group B (all P values <0.01). The image noise of group A ($VMI_{40 \text{ keV}}$) was significantly lower than that in group B (P<0.001).

Subjective image quality evaluation

Table S1 shows the subjective image quality analysis results for group A. In group A, the subjective image noise, contrast, vessel sharpness, and diagnostic image quality of the VMIs at 40 keV were significantly higher than those of $VMIs_{60 \text{ keV}}$, $VMI_{70 \text{ keV}}$, and PCIs (all P values <0.001) but were significantly different from those of VMIs at 50 keV (P>0.05). In group A, there was no significant difference in subjective image quality between the $VMIs_{60 \text{ keV}}$, $VMIs_{70 \text{ keV}}$, and PCIs (all P values >0.05). In group A, there was an overall increase in subjective image noise and vessel

Table 4 Results of objective image quality analysis in group A

Item	PCI	Group A				P value
		40 keV	50 keV	60 keV	70 keV	
ICA						
CT value (HU)	127.17±18.34^	307.11±55.77	213.03±35.55	157.75±23.81	124.80±16.99	<0.001[†]
SNR	20.36 (18.78, 26.67)	46.61 (30.22, 59.44)	39.50 (27.30, 49.76)	34.42 (25.67, 0.13)	30.57 (22.39, 5.18)	<0.001[‡]
CNR	16.74±3.38	55.47±13.43	41.73±9.69	31.58±7.04	24.54±5.24	<0.001[†]
MCA						
CT value (HU)	112.82±17.19^	264.25±48.42	182.48±30.41	134.93±20.28	106.54±14.34	<0.001[†]
SNR	11.16 (7.18, 14.73)	13.66 (9.78, 20.29)	12.18 (9.18, 19.41)	11.63 (9.39, 18.22)	11.16 (9.65, 16.71)	0.052[‡]
CNR	14.08 (12.01, 16.19)	44.48 (36.78, 54.01)	33.03 (28.03, 39.98)	24.51 (22.28, 9.77)	18.95 (16.94, 22.49)	<0.001[‡]
Cerebral parenchyma						
CT value (HU)	28.60 (26.50, 29.4)	31.95 (29.63, 33.68)	29.50 (27.53, 30.88)	27.95 (26.65, 29.08)	27.05 (25.93, 28.38)	<0.001[‡]
Noise (HU)	5.98±0.57	5.08±0.84*[#&]	4.50±0.70	4.20±0.63	4.07±0.58	<0.001[†]

Data are presented as the mean ± standard deviation for normally distributed continuous variables and as the median (interquartile range) for nonnormally distributed continuous variables. Group A: 8 mL of CM with a 1-mL/s flow rate. [†], analysis of variance, [‡], Kruskal-Wallis test. ^, the CT value (ICA or MCA) comparison between VMIs at 70 keV and PCIs (P>0.99 and P=0.567, respectively). *, the noise comparison between VMIs at 40 keV and VMIs at 50 keV, P<0.05; [#], the noise comparison between VMIs at 40 keV and VMIs at 60 keV, P<0.05; [&], the noise comparison between VMIs at 40 keV and VMIs at 70 keV, P<0.05. PCI, polychromatic conventional images; ICA, internal carotid artery; CT, computed tomography; HU, Hounsfield unit; MCA, middle cerebral artery; SNR, signal-to-noise ratio, CNR, contrast-to-noise ratio; CM, contrast media.

sharpness with decreasing VMI level (*Figure 4*). *Table 6* shows the results of the subjective image quality assessment between the VMIs$_{40\,keV}$ in group A and the PCIs in group B. The subjective image noise, contrast, vessel sharpness, and diagnostic image quality in group A (VMI$_{40\,keV}$) were similar to those in group B (PCIs) (all P values >0.05). The interreader agreement for the evaluation of subjective image quality ranged from good to almost perfect consistency, with a κ value ranging from 0.752 to 0.879. *Figure 5* shows a case presentation of cerebral CTA with 8 mL of CM.

Discussion

In this study, we demonstrated the feasibility of using 8 mL of CM and an injection rate of 1 mL/s with VMIs, which provided acceptable image quality for diagnosis on SDCT. VMIs$_{40\,keV}$, which included 8 mL of CM with a 1-mL/s injection rate, demonstrated superior SNR and CNR, along with reduced noise, in comparison to PCIs of routine CM volume and injection rate. To the best of our knowledge, this is the first study to prove the feasibility of using an extremely low CM volume and injection rate in cerebral CTA.

Over recent years, the incidence of CA-AKI after intravenous injection of CM has been a controversial topic. Therefore, other risk factors affecting acute kidney injury must be considered, including severe heart disease, diabetes mellitus, high osmotic pressure, high dose CM, dehydration, and use of nephrotoxic drugs (7,26). In response to these risk factors, the volume and injection rate of CM should be decreased to reduce the risk of CA-AKI. In our pre-experimental study, the CT values of the ICA obtained from 7 mL of CM for cerebral CTA reconstructed from VMIs at 40 keV ranged from 175.5 to 263.7 HU. According to the literature, a CT value of the target vessel ≥200 HU can meet diagnostic requirements (27). Based on this, 7 mL of CM for cerebral CTA could partially meet the diagnostic requirements, and compared to 8 mL of CM, its image noise was higher while its SNR, CNR, and subjective scores were lower. Therefore, using 8 mL of CM may be more appropriate for cerebral CTA examination. Our study used 8 mL of CM and a 1-mL/s injection rate with VMIs$_{40\,keV}$ for cerebral CTA scanning. The average CT value of the ICA was 307.11±55.77 HU, and the average subjective score of the diagnostic quality was 4 [4, 5], which
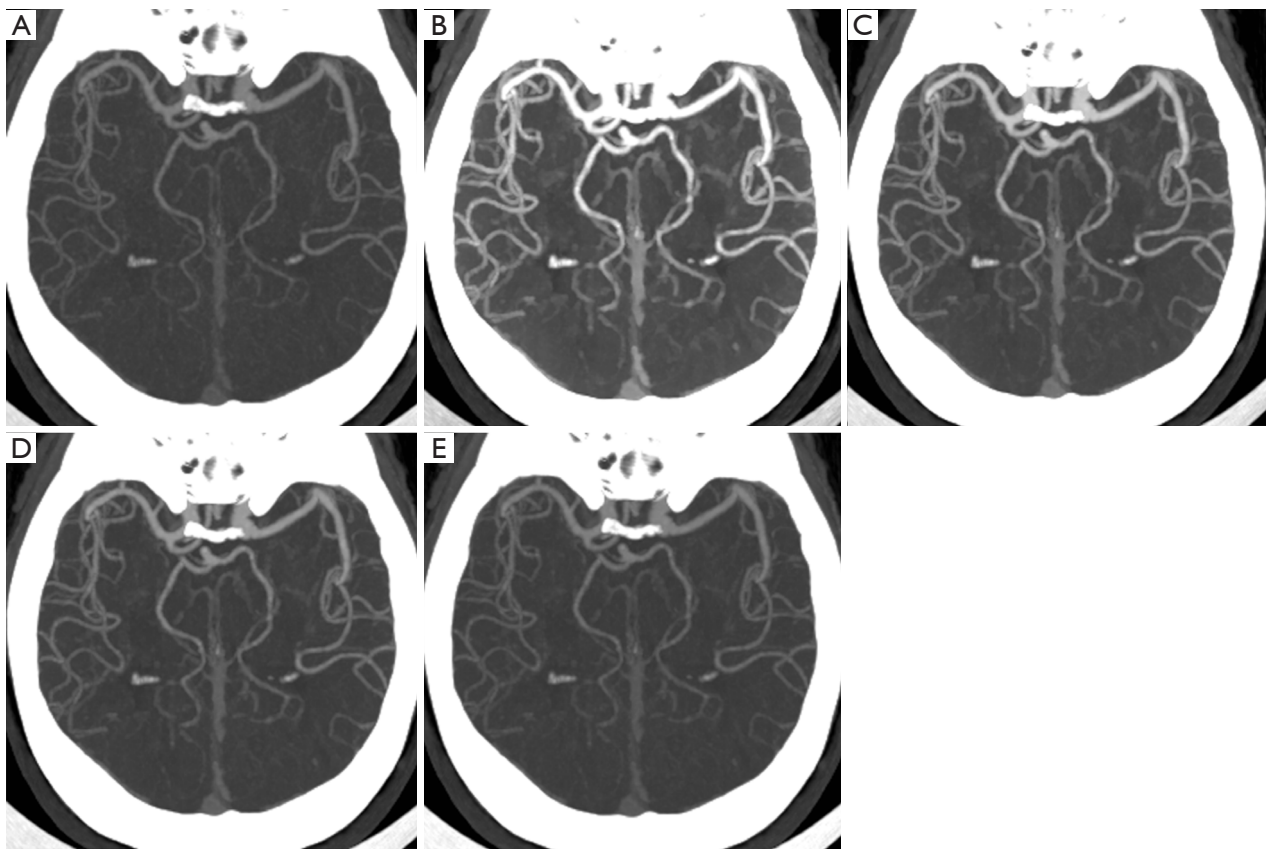
Figure 3 Example maximum intensity projection images of VMIs (40–70 keV) and PCIs in group A. (A) A representative conventional polychromatic image, (B) VMI at 40 keV, (C) VMI at 50 keV, (D) VMI at 60 keV, and (E) VMI at 70 keV. Window settings: level 500 HU and width 1,000 HU. VMI, virtual monoenergetic image; PCI, polychromatic conventional image; HU, Hounsfield unit.

Table 5 Results of objective image quality analysis between group A (40-keV VMIs) and group B (PCIs)

Item	Group A (40-keV VMIs)	Group B (PCIs)	P value
ICA			
CT value (HU)	307.11±55.77	322.07±61.41	0.258[†]
SNR	46.22±20.18	34.32±12.40	0.002[†]
CNR	55.47±13.43	46.18±12.30	0.002[†]
MCA			
CT value (HU)	264.25±48.42	280.25±55.27	0.172[†]
SNR	13.66 [9.78, 20.29]	9.99 [7.53, 14.00]	0.003[‡]
CNR	47.00±12.71	39.45±10.47	0.005[†]
Cerebral parenchyma			
CT value (HU)	31.69±3.03	30.59±2.59	0.084[†]
Noise (HU)	5.08±0.84	6.46±0.88	<0.001[†]

Data are presented as the mean ± standard deviation for normally distributed continuous variables and as the median [interquartile range] for nonnormally distributed continuous variables. Group A: 8 mL of CM with a 1-mL/s flow rate; group B: 40 mL of CM with 4-mL/s flow rate. [†], t-test; [‡], Mann-Whitney test. VMI, virtual monoenergetic image; PCI, polychromatic conventional image; ICA, internal carotid artery; CT, computed tomography; HU, Hounsfield unit; SNR, signal-to-noise ratio, CNR, contrast-to-noise ratio; MCA, middle cerebral artery; CM, contrast media.
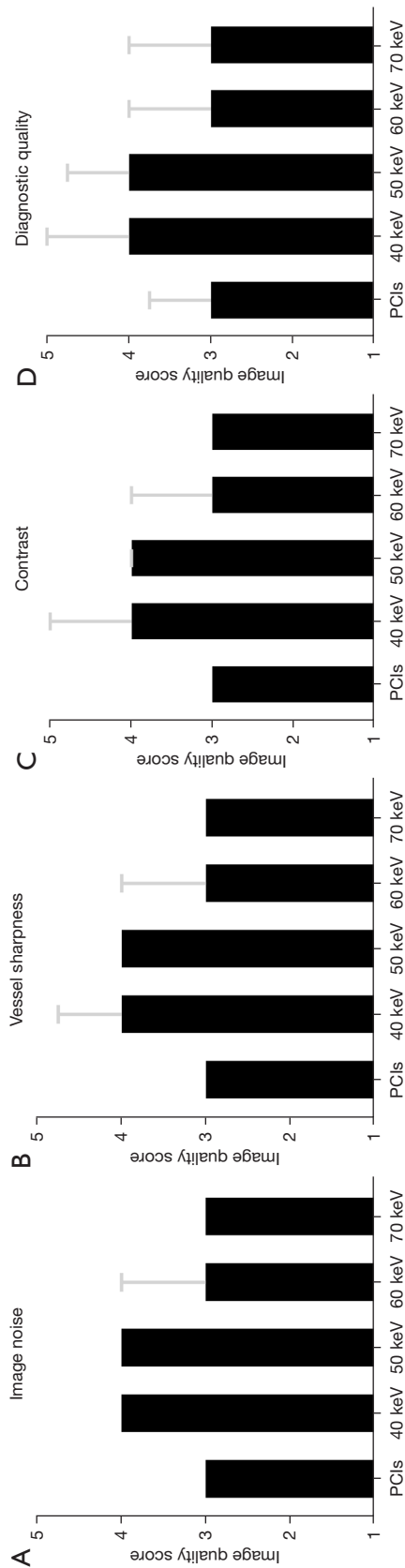
522

Leng et al. Use of 8 mL of iodinated CM in cerebral CT angiography

Figure 4 Results of subjective image quality analysis in group A. Comparison of (A) image noise, (B) vessel sharpness, (C) contrast, and (D) diagnostic image quality for subjective quality evaluation between VMIs at 40–70 keV and PCIs in group A. The image noise, vessel sharpness, contrast, and diagnostic image quality are plotted on the y-axis, while subgroups of group A, including the VMIs at 40–70 keV and PCIs, are plotted on the x-axis. The column bar graph represents the interquartile range of the median subjective score. VMI, virtual monoenergetic image; PCI, polychromatic conventional image.

Table 6 Subjective image quality scores of 40-keV VMIs in group A and PCIs in group B

Measurement by reader	Group A (40-keV VMIs)	Group B (PCIs)	P value
Image noise			
Reader 1	4 [4, 5]	4 [4, 4]	0.546[†]
Reader 2	4 [4, 4.75]	4 [4, 4]	0.879[†]
Kappa value	0.792	0.752	
Vessel sharpness			
Reader 1	4 [4, 5]	4 [4, 5]	0.941[†]
Reader 2	4 [4, 5]	4 [4, 5]	0.832[†]
Kappa value	0.839	0.783	
Contrast			
Reader 1	4 [4, 5]	4 [4, 5]	0.856[†]
Reader 2	4 [4, 5]	4 [4, 5]	0.881[†]
Kappa value	0.834	0.829	
Diagnostic quality			
Reader 1	4 [4, 5]	4 [4, 4.75]	0.808[†]
Reader 2	4 [4, 5]	4 [4, 5]	0.907[†]
Kappa values	0.879	0.778	

Data are presented as the median [interquartile range] for ordinal variables. Group A: 8 mL of CM with a 1-mL/s flow rate; group B: 40 mL of CM with 4-mL/s flow rate. [†], Mann-Whitney test. VMI, virtual monoenergetic image; PCI, polychromatic conventional image; CM, contrast media.

represents diagnostic image quality. Consequently, we believe that the method of using 8 mL of CM for cerebral CTA is feasible.

In clinical practice, it is necessary to optimize the corresponding CM injection scheme. The faster injection rate of CM is, the higher the incidence of CM extravasation and phlebitis. However, patients with low tolerance, such as older adults or those with diabetes or being treated with chemotherapy, are vulnerable due to their thin and fragile peripheral blood vessels, which greatly increases the risk of occurrence (6). One study showed that slow injection can improve the uniformity of CM distribution in blood vessels, thereby improving the quality of imaging (28). As per prior research, complete injection of the contrast agent within a duration of 8 s is recommended (29). In our study, the CM was injected at a rate of 1 mL/s, resulting in the attainment of satisfactory image quality in cerebral CTA. Compared
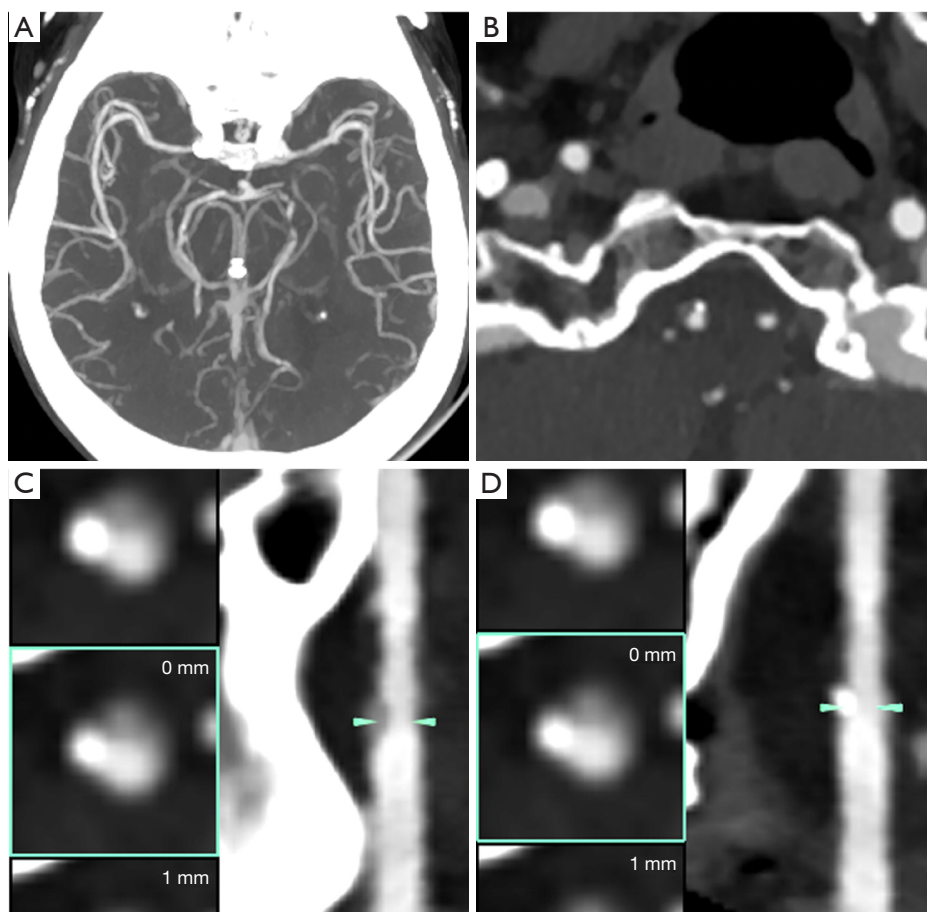
Figure 5 An 81-year-old male from group A (VMI$_{40\text{-keV}}$), subjected to 8 mL of contrast media and an injection rate of 1 mL/s. The mean subjective image quality score of both readers was 5. Images as shown were (A) maximum intensity projection, (B) axial contrast-enhanced CT, and (C,D) probe images, which showed calcified plaques (green arrow) in the intracranial segment of the right vertebral artery accompanied by moderate stenosis of the lumen. Window settings: level 600 HU and width 1,300 HU. VMI, virtual monoenergetic image; CT, computed tomography; HU, Hounsfield unit.

with the conventional 4-mL/s injection rate, the flow rate was reduced by approximately 75%, which allows patients with poor venous access to undergo CTA examination and greatly reduces the risk of venous CM extravasation.

In previous studies, the dose of CM was effectively reduced by decreasing the voltage of X-ray tubes (30,31). However, the use of low tube voltage to decrease CM may lead to an increase in noise, which can compromise the quality of the image and limit its broader clinical application. SDCT mitigates noise by using physics-driven data from the upper and lower layers and employing an anticorrelated noise reduction algorithm while simultaneously maintaining low noise levels across all energy levels of VMIs (21). Several prior investigations have

reported that SDCT can effectively diminish noise and ensure low noise levels across all energy levels, from 40 to 200 keV, for VMIs, thereby significantly enhancing image quality (32,33). Our results indicated that the image noise of VMIs at 40–70 keV was lower than that of PCIs, which is consistent with the abovementioned studies. SDCT combined with low-energy reconstruction techniques can substantially reduce the CM volume in contrast-enhanced CT scans while simultaneously producing images that fulfill clinical requirements (34,35). This preliminary study demonstrated that the subjective image quality scores of VMIs$_{40\text{ keV}}$ with 8 mL of CM were comparable to those of PCIs with a routine CM volume.

The optimal keV of VMI was determined based on the

524

Leng et al. Use of 8 mL of iodinated CM in cerebral CT angiography

overall image quality, including objective and subjective evaluation (19,36,37). Neuhaus *et al.* (19) found that VMIs reconstructed from cerebral CTA at 40 to 45 keV obtained optimal image quality. Our study found that VMIs at 40 keV exhibited higher image noise compared to those at 50 keV, but CT attenuation value, SNR, and CNR were higher at 40 keV than at 50 keV. The subjective image quality scores of VMI at 40 keV were similar to those at 50 keV. In conclusion, 40 keV is the optimal monoenergetic level for VMIs, which is consistent with the above-mentioned research.

There are some limitations to this study. First, this was only a preliminary study, and the experimental design needs further improvement. Second, the experimental group included a fixed CM volume of 8 mL, and personalized scanning was conducted. In the future, the patient's weight should be included to evaluate the dosage of CM. Finally, we only evaluated the image quality of the cerebral CTA and did not evaluate the stenosis and grading caused by vascular calcification plaques. These factors, along with a comparison to digital subtraction angiography, will be included in our further research.

Conclusions

Our study has the feasibility of using 8 mL of CM with a 1-mL/s injection rate on SDCT for cerebral CTA, which could obtain clinically acceptable diagnostic image quality. VMIs$_{40 \text{ keV}}$ represented the optimal reconstruction for clinical application.

Acknowledgments

Footnote

Conflicts of Interest: All authors have completed the ICMJE uniform disclosure form (available at https://qims.amegroups.com/article/view/10.21037/qims-23-914/coif). Y.W. and W.D. are current employees of Philips Healthcare. The other authors have no conflicts of interest to declare.

Ethical Statement: The authors are accountable for all aspects of the work in ensuring that questions related to the accuracy or integrity of any part of the work are appropriately investigated and resolved. The study was conducted in accordance with the Declaration of Helsinki (as revised in 2013) and was approved by the Institutional Review Board of The Second Affiliated Hospital of Nanchang University (examination and approval number review No. 2022 [054]). Informed consent was obtained from all individual participants.

Open Access Statement: This is an Open Access article distributed in accordance with the Creative Commons Attribution-NonCommercial-NoDerivs 4.0 International License (CC BY-NC-ND 4.0), which permits the non-commercial replication and distribution of the article with the strict proviso that no changes or edits are made and the original work is properly cited (including links to both the formal publication through the relevant DOI and the license). See: https://creativecommons.org/licenses/by-nc-nd/4.0/.

References

1. Donmez H, Serifov E, Kahriman G, Mavili E, Durak AC, Menkü A. Comparison of 16-row multislice CT angiography with conventional angiography for detection and evaluation of intracranial aneurysms. Eur J Radiol 2011;80:455-61.

2. Lubicz B, Levivier M, François O, Thoma P, Sadeghi N, Collignon L, Balériaux D. Sixty-four-row multisection CT angiography for detection and evaluation of ruptured intracranial aneurysms: interobserver and intertechnique reproducibility. AJNR Am J Neuroradiol 2007;28:1949-55.

3. Wallace RC, Karis JP, Partovi S, Fiorella D. Noninvasive imaging of treated cerebral aneurysms, Part II: CT angiographic follow-up of surgically clipped aneurysms. AJNR Am J Neuroradiol 2007;28:1207-12.

4. Ki YJ, Kwon SA, Kim HL, Seo JB, Chung WY. The Prevention of Contrast Induced Nephropathy by Sarpogrelate: a Prospective Randomized Controlled Clinical Trial. J Korean Med Sci 2019;34:e261.

5. Mehran R, Dangas GD, Weisbord SD. Contrast-Associated Acute Kidney Injury. N Engl J Med 2019;380:2146-55.

6. Dykes TM, Bhargavan-Chatfield M, Dyer RB. Intravenous contrast extravasation during CT: a national data registry and practice quality improvement initiative. J Am Coll Radiol 2015;12:183-91.

7. Kashani K, Levin A, Schetz M. Contrast-associated acute kidney injury is a myth: We are not sure. Intensive Care Med 2018;44:110-4.

8. Millon D, Derelle AL, Omoumi P, Tisserand M, Schmitt

E, Foscolo S, Anxionnat R, Bracard S. Nontraumatic subarachnoid hemorrhage management: evaluation with reduced iodine volume at CT angiography. Radiology 2012;264:203-9.

9. Chen GZ, Zhang LJ, Schoepf UJ, Wichmann JL, Milliken CM, Zhou CS, Qi L, Luo S, Lu GM. Radiation dose and image quality of 70 kVp cerebral CT angiography with optimized sinogram-affirmed iterative reconstruction: comparison with 120 kVp cerebral CT angiography. Eur Radiol 2015;25:1453-63.

10. Luo S, Zhang LJ, Meinel FG, Zhou CS, Qi L, McQuiston AD, Schoepf UJ, Lu GM. Low tube voltage and low contrast material volume cerebral CT angiography. Eur Radiol 2014;24:1677-85.

11. Chen GZ, Fang XK, Zhou CS, Zhang LJ, Lu GM. Cerebral CT angiography with iterative reconstruction at 70kVp and 30mL iodinated contrast agent: Initial experience. Eur J Radiol 2017;88:102-8.

12. Mu R, Meng Z, Guo Z, Qin X, Huang G, Yang X, Jin H, Yang P, Zhang X, Zhu X. Dual-layer spectral detector computed tomography parameters can improve diagnostic efficiency of lung adenocarcinoma grading. Quant Imaging Med Surg 2022;12:4601-11.

13. Rassouli N, Etesami M, Dhanantwari A, Rajiah P. Detector-based spectral CT with a novel dual-layer technology: principles and applications. Insights Imaging 2017;8:589-98.

14. Kalisz K, Rassouli N, Dhanantwari A, Jordan D, Rajiah P. Noise characteristics of virtual monoenergetic images from a novel detector-based spectral CT scanner. Eur J Radiol 2018;98:118-25.

15. Hickethier T, Baeßler B, Kroeger JR, Doerner J, Pahn G, Maintz D, Michels G, Bunck AC. Monoenergetic reconstructions for imaging of coronary artery stents using spectral detector CT: In-vitro experience and comparison to conventional images. J Cardiovasc Comput Tomogr 2017;11:33-9.

16. Doerner J, Hauger M, Hickethier T, Byrtus J, Wybranski C, Große Hokamp N, Maintz D, Haneder S. Image quality evaluation of dual-layer spectral detector CT of the chest and comparison with conventional CT imaging. Eur J Radiol 2017;93:52-8.

17. Ananthakrishnan L, Rajiah P, Ahn R, Rassouli N, Xi Y, Soesbe TC, Lewis MA, Lenkinski RE, Leyendecker JR, Abbara S. Spectral detector CT-derived virtual non-contrast images: comparison of attenuation values with unenhanced CT. Abdom Radiol (NY) 2017;42:702-9.

18. Sakabe D, Funama Y, Taguchi K, Nakaura T, Utsunomiya D, Oda S, Kidoh M, Nagayama Y, Yamashita Y. Image quality characteristics for virtual monoenergetic images using dual-layer spectral detector CT: Comparison with conventional tube-voltage images. Phys Med 2018;49:5-10.

19. Neuhaus V, Große Hokamp N, Abdullayev N, Maus V, Kabbasch C, Mpotsaris A, Maintz D, Borggrefe J. Comparison of virtual monoenergetic and polyenergetic images reconstructed from dual-layer detector CT angiography of the head and neck. Eur Radiol 2018;28:1102-10.

20. Huang X, Gao S, Ma Y, Lu X, Jia Z, Hou Y. The optimal monoenergetic spectral image level of coronary computed tomography (CT) angiography on a dual-layer spectral detector CT with half-dose contrast media. Quant Imaging Med Surg 2020;10:592-603.

21. Tsang DS, Merchant TE, Merchant SE, Smith H, Yagil Y, Hua CH. Quantifying potential reduction in contrast dose with monoenergetic images synthesized from dual-layer detector spectral CT. Br J Radiol 2017;90:20170290.

22. Oda S, Takaoka H, Katahira K, Honda K, Nakaura T, Nagayama Y, Taguchi N, Kidoh M, Utsunomiya D, Funama Y, Noda K, Oshima S, Yamashita Y. Low contrast material dose coronary computed tomographic angiography using a dual-layer spectral detector system in patients at risk for contrast-induced nephropathy. Br J Radiol 2019;92:20180215.

23. Ren H, Zhen Y, Gong Z, Wang C, Chang Z, Zheng J. Feasibility of low-dose contrast media in run-off CT angiography on dual-layer spectral detector CT. Quant Imaging Med Surg 2021;11:1796-804.

24. Sodickson AD, Keraliya A, Czakowski B, Primak A, Wortman J, Uyeda JW. Dual energy CT in clinical routine: how it works and how it adds value. Emerg Radiol 2021;28:103-17.

25. International Commission on Radiological Protection. Conversion coefficients for use in radiological protection against external radiation. ICRP Publication 74, Ann. 1997; ICRP 26(3-4).

26. James MT, Samuel SM, Manning MA, Tonelli M, Ghali WA, Faris P, Knudtson ML, Pannu N, Hemmelgarn BR. Contrast-induced acute kidney injury and risk of adverse clinical outcomes after coronary angiography: a systematic review and meta-analysis. Circ Cardiovasc Interv 2013;6:37-43.

27. Chen Y, Zhang X, Xue H, Zhu Y, Wang Y, Li Y, Zhang Z, Jin Z. Head and neck angiography at 70 kVp with a third-generation dual-source CT system in patients: comparison with 100 kVp. Neuroradiology 2017;59:1071-81.

526

Leng et al. Use of 8 mL of iodinated CM in cerebral CT angiography

28. Kalra MK, Becker HC, Enterline DS, Lowry CR, Molvin LZ, Singh R, Rybicki FJ. Contrast Administration in CT: A Patient-Centric Approach. J Am Coll Radiol 2019;16:295-301.

29. Feng R, Tong J, Liu X, Zhao Y, Zhang L. High-Pitch Coronary CT Angiography at 70 kVp Adopting a Protocol of Low Injection Speed and Low Volume of Contrast Medium. Korean J Radiol 2017;18:763-72.

30. Liu B, Gao S, Chang Z, Wang C, Liu Z, Zheng J. Lower extremity CT angiography at 80 kVp using iterative model reconstruction. Diagn Interv Imaging 2018;99:561-8.

31. Kayan M, Demirtas H, Türker Y, Kayan F, Çetinkaya G, Kara M, Orhan Çelik A, Umul A, Yılmaz Ö, Recep Aktaş A. Carotid and cerebral CT angiography using low volume of iodinated contrast material and low tube voltage. Diagn Interv Imaging 2016;97:1173-9.

32. Sellerer T, Noël PB, Patino M, Parakh A, Ehn S, Zeiter S, Holz JA, Hammel J, Fingerle AA, Pfeiffer F, Maintz D, Rummeny EJ, Muenzel D, Sahani DV. Dual-energy CT: a phantom comparison of different platforms for abdominal imaging. Eur Radiol 2018;28:2745-55.

33. Große Hokamp N, Gilkeson R, Jordan MK, Laukamp KR, Neuhaus VF, Haneder S, Halliburton SS, Gupta A. Virtual monoenergetic images from spectral detector CT as a surrogate for conventional CT images: Unaltered attenuation characteristics with reduced image noise. Eur J Radiol 2019;117:49-55.

34. Carrascosa P, Leipsic JA, Capunay C, Deviggiano A, Vallejos J, Goldsmit A, Rodriguez-Granillo GA. Monochromatic image reconstruction by dual energy imaging allows half iodine load computed tomography coronary angiography. Eur J Radiol 2015;84:1915-20.

35. Raju R, Thompson AG, Lee K, Precious B, Yang TH, Berger A, Taylor C, Heilbron B, Nguyen G, Earls J, Min J, Carrascosa P, Murphy D, Hague C, Leipsic JA. Reduced iodine load with CT coronary angiography using dual-energy imaging: a prospective randomized trial compared with standard coronary CT angiography. J Cardiovasc Comput Tomogr 2014;8:282-8.

36. Fransson V, Mellander H, Ramgren B, Andersson H, Arena F, Ydström K, Ullberg T, Wassélius J. Image quality of spectral brain computed tomography angiography using halved dose of iodine contrast medium. Neuroradiology 2023;65:1333-42.

37. Ghadri JR, Küest SM, Goetti R, Fiechter M, Pazhenkottil AP, Nkoulou RN, Kuhn FP, Pietsch C, von Schulthess P, Gaemperli O, Templin C, Kaufmann PA. Image quality and radiation dose comparison of prospectively triggered low-dose CCTA: 128-slice dual-source high-pitch spiral versus 64-slice single-source sequential acquisition. Int J Cardiovasc Imaging 2012;28:1217-25.

Table S1 Results of subjective image quality analysis in group A

Item	PCIs	Group A				P value
		40 keV	50 keV	60 keV	70 keV	
Image noise	3 [3, 3]	4 [4, 4]	4 [4, 4]	3 [3, 4]	3 [3, 3]	<0.001[†]
Vessel sharpness	3 [3, 3]	4 [4, 4.75]	4 [4, 4]	3 [3, 4]	3 [3, 3]	<0.001[†]
Contrast	3 [3, 3]	4 [4, 5]	4 [3.25, 4]	3 [3, 4]	3 [3, 3]	<0.001[†]
Diagnostic quality	3 [3, 3.75]	4 [4, 5]	4 [4, 4.75]	3 [3, 4]	3 [3, 4]	<0.001[†]
Overall image quality	3 [3, 3.75]	4 [4, 5]	4 [4, 4.75]	3 [3, 4]	3 [3, 4]	<0.001[†]

Data are presented as the median [interquartile range] for ordinal variables. Group A: 8 mL of CM with a 1-mL/s flow rate; group B: 40 mL of CM with 4-mL/s flow rate. [†], Kruskal-Wallis test. PCI, polychromatic conventional image; CM, contrast media.